



Characteristic Trigonometric Function Application to the Direct Variation Method for Clamped, Simply and Freely Supported Plate Under Uniform Load Distributions

Okeke Thompson Edozie^a, Onyeka Festus Chukwudi^b, Nwa-David Chidobere^c

^aDepartment of Civil Engineering, University of Nigeria, Nsukka, Enugu State, 410101, Nigeria.

^bDepartment of Civil Engineering, Edo State University Uzairue, Edo State, 312102, Nigeria.

^cDepartment of Civil Engineering, Michael Okpara University of Agriculture, Umudike, Abia State, 440109, Nigeria.

* Corresponding author: Nwa-David Chidobere David, nwadaid.chidobere@mouau.edu.ng

ARTICLE INFORMATION

Article history:

Received 21 August 2022

Revised 08 September 2022

Accepted 10 September 2022

Available online 9 Oct. 2022

Keywords:

3-D plate theory, Exact bending solution, CSFS thick Plate, Trigonometric Displacement Functions

ABSTRACT

In this paper, the bending attributes of a uniformly loaded three-dimensional (3-D) plate are modelled using exact trigonometric shape functions; the effects of shear correction factors associated with refined plate theory (RPT) are obviated. As an advancement of the RPT theory, the equations of equilibrium of the current model were obtained from fundamental principles of elasticity by applying the three-dimensional (3-D) kinematic deformation and constitutive relations which results of the six stress components. The formulated 3-D kinematics and constitutive relations was used to obtain the energy equation which was later transformed into compatibility equation to determine the function of deflection and rotation. The governing equations were obtained and solved in terms of trigonometry to get the exact deflection function of the plate. The rotation and deflection function were substituted into the energy equation to get the coefficients of deflection and rotation. Thereafter, these coefficients were substituted into the obtained displacement and stress equations to get the model for evaluating the bending of thick plates that was clamped on the first edge, free at the third edge, with the second and fourth edges simply supported respectively (CSFS). The recorded outcome confirms that the values for stresses and displacement obtained from this 3-D theory is more accurate and reliable compared to refined plate theories applied in previous studies. The overall average percentage differences between the present study and the studies by Onyeka (2021) and Gwarah (2019) for center deflection of a square plate was 4.8%. This showed about 95% confidence level for adoption of 3-D plate analogy which is required as the only reliable modeling theory for an exact bending solution of thick plates as unrealistic solutions are obtained from 2D shear deformation theories.

1. Introduction

Thick plates are three-dimensional (3D) structural elements with extensive application in aeronautical, mechanical and structural engineering. [1-3]; due to their cost benefits, lightweight,

ability to be tailored to desired structural properties and load resistance characteristics [4]. In structural engineering, they are largely used in foundation footings, ship hulls, bulkheads, water tanks, spacecraft panels, bridge deck slabs, roof and floor slabs [5-7]. Analyzing the attributes and failure conditions of thick plates is necessary to ensure safer, more economical designs and to maximize their properties.

The edges of thick plates have different boundary conditions which can be free, simply supported, or clamped. Plates can be circular, triangular, elliptical, skew or rectangular in shape. They can be orthotropic, anisotropic, or isotropic based on their material properties and deformation nature [8-9]. Isotropic plates are plates with the same properties of the material at a point in all directions while anisotropic plates have different properties of the material at a point in all directions. When anisotropic plate consists of three mutually-perpendicular planes of symmetry with regard to its elastic properties, it is considered as orthotropic [10]. Plates are also categorized as thin, moderately thick, or thick according to their thickness [11-14]. The thick rectangular isotropic plate is considered in this study.

Thick plates can be subjected to evenly distributed loads and transverse loads on the plates' mid-plane. A plate is considered to be of uniformly distributed load when it is subjected to an applied load at the boundary perpendicular to the mid-surface and distributed through the plate's thickness [15]. The plates become elastically deformed as a result of these loadings. Without proper management, plate bending can result in structural failure. Hence, it is of paramount importance to study and analyze the bending of plates in order to obviate its failure.

To analyze the bending of thick plates, series of theories such as the classical plate theory (CPT), refined plate theories (RPT), and three-dimensional (3D) elasticity theory; have been developed and employed. The CPT which is also known as the Kirchhoff plate theory [16], is the simplest plate theory. In CPT, transverse shear stresses along the thickness axis are not considered and are therefore not suitable for resolving thick plates. RPT comprises of the first-order shear deformation theory (FSDT) [17, 18] and the higher-order shear deformation theories (HSDTs) [19, 20].

The continuous transverse shear stress along the plate thickness is considered in FSDT but it is inconsistent with the zero stress conditions on free surfaces, and for reliable results to be obtained, shear correction factor is applied. HSDTs were designed to overcome the use of correction factors and solve the issue of free surfaces. Basically, the thick plate analysis is a three-dimensional problem and only approximations of the true 3-D equations of elasticity can result from 2-D refined plate theories [21-23].

However, researchers did not do a lot of work on 3D thick plate analysis with a view to obtain the realistic expression for calculating the deflection and stresses of the plate through minimizations with respect to the rotations and deflection coefficients obtained as the result of the governing equation. This literature blank is worth completing and validates the necessity of this work.

The study of the bending characteristics of thick plates can be accomplished through either numerical, analytical, energy approach or a blend of any [22, 24]. Numerical methods applied by different scholars in [25-27], often give approximate solutions to the plate bending problem and they include boundary element, finite difference, Galerkin, Ritz, Bubnov-Galerkin, Collocation, truncated double Fourier series and Kantorovich methods.

Analytical methods as used in [15,28,29], solves the plate problems satisfying the support conditions of the plate in the governing equations with the various points of the surface of the plate. Method of integral transforms, methods of Eigen expansion, Navier and Levy series are different forms of analytical method [30]. Energy method can be in analytical or numerical form, although its total energy is equivalent to the sum of all the strain energy and potential energy or external work on the

continuum [31]. This study employs an energy method in an analytical form to fix the bending of thick plates.

An analytical improved plate theory is presented in this study for investigating the exact bending behavior of a three-dimensional plate under uniformly distributed load using trigonometric displacement functions and direct variation technique. Unlike most studies, this study considers the deflection, shear stresses along the x-y axis, x-z axis, y-z axis, the normal stresses along x, y, z coordinates produced due to the applied load on the plate, and the in-plane displacement in the direction of x and y co-ordinates. The veracity of thick plate analysis, largely depends on the precision of the displacement functions and this is a major concern for engineers. Assumed displacement functions which often yield approximate solutions, have been used by most scholars to rectify the bending problem [32]. This study covers this gap in that its displacement function are exactly as they are derived from the governing equation using an analytical approach, including the application of trigonometric functions which offers a closer form solution than those of the polynomials [33, 34].

1.2 Review of Previous Studies

Shetty *et al.*, [35] applied a simple plate theory in the third order displacement field, in which just one unknown variable displacement was used for absolute formulation of thick plates. Plates with simply-supported edges were considered in their study. Their result was corresponding to those of CPT and also consistent with the deflection outcome of FSDTs and HSDTs. But they failed to employ the 3D plate theory, which gives a close-form solution for typical three-dimensional thick plates. The authors also could not analyze thick plates with CSFS boundary condition.

Bhaskar *et al.*, [36] developed a finite element solution for bi-directional bending assessment of thick isotropic plates using MATLAB code based on a new inverse TSDT. The transverse shear deflection and rotating inertia effects were taken into account. The governing equations and boundary conditions of the theory was derived from dynamic version of the virtual work principle. When compared to other HSDTs, their model gave precise predictions of stresses and displacements. However, they failed to consider an analytical approach and CSFS thick plates. A 3-D investigation was not captured in their analysis.

RPT with exponential functions was used by Sayyad and Ghugal [37] to analyze the displacements and stresses of plates with the SSSS boundary condition. The results obtained were satisfactory compared with other refined plate theories even without using correction factors. A 3 D theory and trigonometric function were not engaged in their analysis. Their study did not take CSFS plates into consideration.

Mantari and Soares [38] used HSDT to obtain a Navier-type analytical solution of the governing equations of simply supported plates under transverse bi-sinusoidal loads, with an assumption of variation for the mechanical features of the plates in the thickness axis. Principle of virtual work was employed in their study and was verified to be accurate when compared with other shear deformation trigonometric theory. Plates with uniformly distributed loads and CSFS support conditions were not considered. Their study could not include all the stresses and strains in the plate as it neglected the strain and stress along the thickness direction, hence considered as an incomplete three-dimensional (3-D) analytical approach.

Tash and Neya [39] utilized displacement potential functions to examine the bending of isotropic thick plates that are transversely simply supported, with thickness variations. The governing equations which were of quadratic and fourth order, were solved using a variable separation method with the exact support conditions satisfied. They verified their solution with the finite element

method and it proved satisfactory. Trigonometric displacement functions were not employed and plates with CSFS boundary conditions were neglected.

Based on Levy's approach and two-variable RPT, Thai and Choi [40] obtained an analytical solution for the bending of thick rectangular plates with two simply-supported opposite edges and the other two edges having arbitrary edge conditions; satisfying the zero boundary conditions on the plates' surfaces neglecting the shear correction factors. The predictions of CPT, FSDT, and TSDT was consistent with their results. Their solution is inexact as it failed to capture the entire stresses in the plate. There was no consideration for CSFS thick plates.

Zhong and Xu [41] combined decoupling method to the modified Navier's solution to study the bending behavior of thick plates with all edges clamped. The main governing equations applied in their study were based on Mindlin's HSDT. The three coupled governing equations were modified to independent partial differential equations that can be solved individually employing a new function and analytic solutions were derived from the solutions of the decoupled equations. Although their approach does not need complex matrix derivations for calculating the coefficients, their solution is incomplete because of the absence of 3-D plate theory. Plates with CSFS boundary conditions were not addressed.

Ghugal and Gajbhiye [42] conducted a bending study using RPT with Virtual work principle. Without using the shear correction factor associated with FSDTs, the shear and strain deformation effect was considered. Due to the analytical approach employed, closed-form solutions that are very close to exact 3-D solutions were obtained. The condition of the zero shear transverse stresses was satisfactory. Trigonometric functions and three-dimensional plate theory were not considered and plates with CSFS support conditions were not covered.

Satisfying the zero-shear-stress condition on the plate surfaces, the displacements and stresses of a rectangular thick plate with different span-to-depth ratio was presented by Ibearugbulem *et al.* [43] using a variational method and the polynomial function. Their study could not include all the stresses in the plate and failed to apply trigonometric function. The authors didn't cover plates with CSFS edge condition.

Although Onyeka [44] adopted direct variation approach to present the effect of stress and load distribution analysis for plates with one clamped edge, free at the other and the two other opposite edges simply-supported (CSFS) using HSDT, trigonometric functions and three-dimensional plate theory were not considered. The author developed a model for calculating the critical lateral imposed load of the plate without considering all the stress components. This limitation was addressed in this study.

Ezeh et al. (2018) [45] applied the direct variation energy approach to obtain displacement coefficients without the need for correction factor for CCCS and SSFS plates. They employed 2D theory with polynomial shape function for their analysis and their solutions were adequate compared with the outcome of previous papers. They failed to include CSFS plates and trigonometric function. All the six stress elements of the plate were not considered in their study.

Onyeka and Okeke [23] used trigonometric shape functions and an exact 3-D plate theory to derive the exact displacement and stress solutions of a thick plate subjected to a uniform distributed load. The energy equation of the CCFC plate was formulated using the kinematics and three-dimensional constitutive relations for static elasticity theory, established on the general thick plate assumption. Plates with CSFS boundary condition were not taken into account.

The bending of SSSS 3-D thick plates was investigated by Ibearugbulem *et al.* [46] by means of analytical method with exact polynomial functions obtained from the governing equation. The total potential-energy functional was obtained with the six strains and stress components. When the values obtained from stress and deflection were set side by side with those of RPT, the coarseness of RPT for thick plate analysis, was divulged. Exact trigonometric function was not employed in their analysis and plates with CSFS support conditions were not covered.

Onyeka and mama [21], Onyeka *et al.*, [22], employed the variational technique using exact trigonometric function and 3D plate theory to analyze the bending behavior of thick plates. In [21], SSSS plates were considered while [22] covered plates with CSCS support conditions. Both authors presented their numerical solution and compared the calculated values of deflection and stresses with CPT and 2D-RPT, which confirmed the inadequacy of these other theories for evaluation of thick plates. But they failed to address plates with CSFS boundary condition.

Based on the 3-D theory of elasticity, Grigorenko *et al.*, (2013) [47] employed a numerical approach to obtain the bending solutions of a thick plate. The method of spline collocation in two coordinate directions was used for their analysis. They determined the displacements and stresses in plates with clamped support conditions. Their numerical approach cannot evaluate the deflection value at any given point in the plate and they failed to take into account plates with CSFS edge condition.

Prior studies have demonstrated that the displacement function used by most authors is assumed. The shape functions were not derived from the governing compatibility equation that was obtained from the first principle and this makes their analysis unreliable. Erroneous assumptions as regards the kinematics of deformation were made by the 2-D theories (incomplete 3-D theory) used by previous researchers, which produced in exact solutions. Previous studies except [21, 22, 46, 47], did not address exact 3-D models for the thick plate bending analysis. This gap is also addressed in this study.

In this study, a 3-D plate theory was developed and applied in the thick plate carrying a uniformly distributed compressive load. The focus of this work is to study the exact 3-D bending analysis of thick rectangular plates clamped at the first edge, free at the third edge, with the second and fourth edges simply supported respectively (CSFS) by finding out the coefficient of deflection and shear deformation of the plate through the three governing equations developed using the direct variational energy method.

2. Methodology

2.1 Model Formulation

The research methodology of this study is presented by considering a rectangular plate in the Figure 1 as a three-dimensional element in which the deformation exists in the three axis: length (a), width (b) and thickness (t). The analytical approach of energy method was used to obtain formulas for the analysis. The 3-D kinematics and constitutive relations for a static elastic theory of plate was used to formulate the governing equations which enables development of the formulae for the analysis.

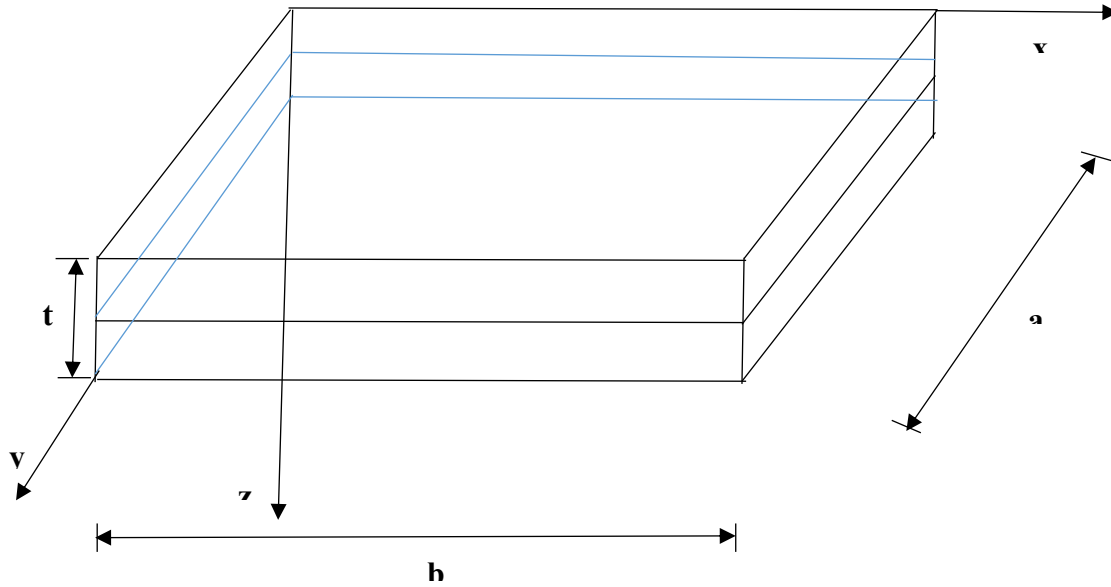


Figure 1: An element of thick rectangular plate showing middle surface

2.2 Kinematics

The kinematics of the study was formulated by taking the assumption of the plate that the x-z section and the y-z section, is no longer normal to x-y plane after bending. Thus, the 3-D displacement kinematics along x, y and z axis are obtained in line with the work of Onyeka *et al.* [2], as:

$$p = z \cdot \phi_x \quad (1)$$

$$q = z \cdot \phi_y \quad (2)$$

Given that:

$$z = kt \quad (3)$$

$$\beta = \frac{a}{t} \quad (4)$$

$$\gamma = \frac{b}{a} \quad (5)$$

Thus, the six non-dimensional coordinates strain components were derived using strain-displacement expression according to Hooke's law and presented in Equation (6) - (11):

$$\varepsilon_x = \frac{1}{a} \cdot \frac{\partial p}{\partial u} \quad (6)$$

$$\varepsilon_y = \frac{1}{a\gamma} \cdot \frac{\partial q}{\partial v} \quad (7)$$

$$\varepsilon_z = \frac{1}{t} \cdot \frac{\partial U}{\partial k} \quad (8)$$

$$\gamma_{xy} = \frac{1}{a} \cdot \frac{\partial q}{\partial u} + \frac{1}{a\gamma} \cdot \frac{\partial p}{\partial v} \quad (9)$$

$$\gamma_{xz} = \frac{1}{a} \cdot \frac{\partial U}{\partial u} + \frac{1}{t} \cdot \frac{\partial p}{\partial k} \quad (10)$$

$$\gamma_{yz} = \frac{1}{a\gamma} \cdot \frac{\partial U}{\partial v} + \frac{1}{t} \cdot \frac{\partial q}{\partial k} \quad (11)$$

2.3. Constitutive Relations

The three-dimensional constitutive relation for isotropic material is given as:

$$\begin{bmatrix} \epsilon_x \\ \epsilon_y \\ \epsilon_z \\ \gamma_{xz} \\ \gamma_{yz} \\ \gamma_{xy} \end{bmatrix} = \frac{1}{E} \begin{bmatrix} 1 & -\mu & -\mu & 0 & 0 & 0 \\ -\mu & 1 & -\mu & 0 & 0 & 0 \\ -\mu & -\mu & 1 & 0 & 0 & 0 \\ 0 & 0 & 0 & 2(1+\mu) & 0 & 0 \\ 0 & 0 & 0 & 0 & 2(1+\mu) & 0 \\ 0 & 0 & 0 & 0 & 0 & 2(1+\mu) \end{bmatrix} \begin{bmatrix} \sigma_x \\ \sigma_y \\ \sigma_z \\ \tau_{xz} \\ \tau_{yz} \\ \tau_{xy} \end{bmatrix} \quad (12)$$

The six stress components were obtained by substituting Equations 6 to 11 into Equation 12 and simplifying the outcome gave:

$$\sigma_x = \left[\mu \frac{kt}{\gamma a} * \frac{\partial \phi_y}{\partial v} + (1-\mu) \frac{kt}{a} * \frac{\partial \phi_x}{\partial u} + \mu \frac{1}{t} * \frac{\partial U}{\partial k} \right] \frac{E}{(1+\mu)(1-2\mu)} \quad (13)$$

$$\sigma_y = \left[\mu kt * \frac{\partial \phi_x}{a \partial u} + \frac{\mu}{t} * \frac{\partial U}{\partial k} + \frac{(1-\mu)kt}{\gamma a} * \frac{\partial \phi_y}{\partial v} \right] \frac{E}{(1+\mu)(1-2\mu)} \quad (14)$$

$$\sigma_z = \left[\frac{\mu kt}{\gamma a} * \frac{\partial \phi_y}{\partial v} + \frac{(1-\mu)}{t} * \frac{\partial U}{\partial k} + \mu kt * \frac{\partial \phi_x}{a \partial u} \right] \frac{E}{(1+\mu)(1-2\mu)} \quad (15)$$

$$\tau_{xy} = \left[\frac{kt \partial \phi_y}{a 2 \partial u} * \frac{kt}{2 \gamma a} \frac{\partial \phi_x}{\partial v} \right] \frac{E(1-2\mu)}{(1+\mu)(1-2\mu)} \quad (16)$$

$$\tau_{yz} = \left[\frac{1}{a 2 \gamma} \frac{\partial U}{\partial Q} + \frac{\phi_y}{2} \right] \frac{(1-2\mu)E}{(1+\mu)(1-2\mu)} \quad (17)$$

$$\tau_{xz} = \left[\frac{1}{a} \frac{\partial U}{2 \partial u} + \frac{\phi_x}{2} \right] \frac{(1-2\mu)E}{(1+\mu)(1-2\mu)} \quad (18)$$

2.4 Formulation of Energy

The potential energy which is summation of all the external work done on the body of the material and strain energy generated due to the applied load on the plate is mathematically defined as:

$$\mathcal{A} = \mathcal{E} - \mathcal{W} \quad (19)$$

Given that;

$$\mathcal{W} = wab \cap \int_0^1 \int_0^1 C \, du \, dv \quad (20)$$

And;

$$\epsilon = \frac{tab}{2} \int_0^1 \int_0^1 \int_{-0.5}^{0.5} (\sigma_x \epsilon_x + \sigma_y \epsilon_y + \sigma_z \epsilon_z + \tau_{xy} \gamma_{xy} + \tau_{xz} \gamma_{xz} + \tau_{yz} \gamma_{yz}) du dv dk \quad (21)$$

Substituting Equations 22 and 25 into Equation 24 to get the energy equation as:

$$\begin{aligned} \mathcal{A} = & \frac{Et^3\gamma}{24(1+\mu)(1-2\mu)} \int_0^1 \int_0^1 \left[\left(\frac{\partial \phi_y}{\partial u} \right)^2 \frac{(1-2\mu)}{2} + \frac{1}{\gamma} \frac{\partial \phi_x}{\partial u} * \frac{\partial \phi_y}{\partial v} + \frac{(1-\mu)}{\gamma^2} \left(\frac{\partial \phi_y}{\partial v} \right)^2 \right. \\ & + \frac{(1-\mu)}{t^2} * \left(\frac{\partial U}{\partial k} \right)^2 \beta^2 + \frac{(1-2\mu)}{2\gamma^2} \left(\frac{\partial \phi_x}{\partial v} \right)^2 \\ & + \frac{6(1-2\mu)}{t^2} \left\{ a^2 \phi_x^2 + \left(\frac{\partial U}{\partial u} \right)^2 + a^2 \phi_y^2 + \left(\frac{\partial U}{\partial v} \right)^2 \frac{1}{\gamma^2} + a \left(\frac{\partial U}{\partial u} \right) 2\phi_x \right. \\ & \left. \left. + \left(\frac{\partial U}{\partial v} \right) 2a * \frac{\phi_y}{\gamma} \right\} + \left(\frac{\partial \phi_x}{\partial u} \right)^2 (1-\mu) \right] du dv - w\gamma a^2 \int_0^1 \int_0^1 CS du dv \end{aligned} \quad (22)$$

2.5. Solution to the Equilibrium Equation

The two compatibility equations were obtained by minimizing the total potential energy functional with respect to rotations in x-z and in y-z plane to give:

$$\begin{aligned} \frac{Et^3\gamma}{24(1+\mu)(1-2\mu)} \int_0^1 \int_0^1 \left[2(1-\mu) \frac{\partial^2 \phi_x}{\partial u^2} + \frac{\partial^2 \phi_y}{\partial u \partial v} * \frac{1}{\gamma} + \frac{(1-2\mu)}{\gamma^2} \frac{\partial^2 \phi_x}{\partial v^2} \right. \\ \left. + \left(2a^2 \theta_{sx} + 2a \frac{\partial U}{\partial u} \right) \frac{6(1-2\mu)}{t^2} \right] du dv = 0 \end{aligned} \quad (23)$$

$$\begin{aligned} \frac{Et^3\gamma}{24(1+\mu)(1-2\mu)} \int_0^1 \int_0^1 \left[\frac{\partial^2 \phi_x}{\partial u \partial v} * \frac{1}{\gamma} + 2 \frac{\partial^2 \phi_y}{\partial v^2} * \frac{(1-\mu)}{\gamma^2} + 2 \frac{(1-2\mu)}{2} \frac{\partial^2 \phi_y}{\partial u^2} \right. \\ \left. + \left(2a^2 \phi_y + \frac{2a}{\gamma} \frac{\partial U}{\partial v} \right) \frac{6(1-2\mu)}{t^2} \right] du dv = 0 \end{aligned} \quad (24)$$

The solution of the equilibrium differential equation gives the characteristics trigonometric displacement and rotation functions as presented in the Equation 25-27 as:

$$U = [1 \quad u \quad \cos(uc_1) \quad \sin(uc_1)] \begin{bmatrix} a_0 \\ a_1 \\ a_2 \\ a_3 \end{bmatrix} \cdot [1 \quad v \quad \cos(vc_1) \quad \sin(vc_1)] \begin{bmatrix} b_0 \\ b_1 \\ b_2 \\ b_3 \end{bmatrix} \quad (25)$$

$$\phi_x = \frac{c}{a} \cdot H_0 \cdot [1 \quad c_1 \sin(uc_1) \quad c_1 \cos(uc_1)] \begin{bmatrix} a_1 \\ a_2 \\ a_3 \end{bmatrix} \cdot [1 \quad v \quad \cos(vc_1) \quad \sin(vc_1)] \begin{bmatrix} b_0 \\ b_1 \\ b_2 \\ b_3 \end{bmatrix} \quad (26)$$

$$\phi_y = \frac{c}{a\beta} \cdot H_0 \cdot [1 \quad u \quad \cos(uc_1) \quad \sin(uc_1)] \begin{bmatrix} a_0 \\ a_1 \\ a_2 \\ a_3 \end{bmatrix} \cdot [1 \quad c_1 \sin(vc_1) \quad c_1 \cos(vc_1)] \begin{bmatrix} b_1 \\ b_2 \\ b_3 \end{bmatrix} \quad (27)$$

Considering a transversely loaded rectangular thick plate whose Poisson's ratio is 0.3 under uniformly distributed load as shown in the Figure 2, the derived trigonometric deflection functions is subjected to a CSFS boundary condition to get the particular solution of the deflection functions is subjected to a CSFS boundary condition to get the particular solution of the deflection.

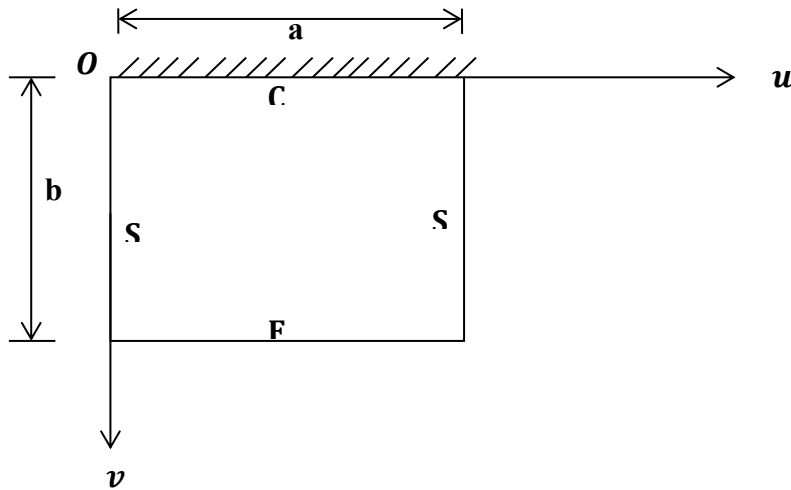


Figure 2: CSCS Rectangular Plate

Applying the initial conditions of the plate in Figure 2, the relationship between the displacement and shape function of the plate as:

$$U = C \cdot \eta \quad (28)$$

$$\phi_x = \frac{h}{a} \cdot \frac{\partial C}{\partial u} \quad (29)$$

$$\phi_y = \frac{g}{\gamma a} \cdot \frac{\partial C}{\partial v} \quad (30)$$

The in trigonometric form of the shape function of the plate after satisfying the boundary conditions is given as:

$$C = (\sin \pi u) \cdot \left(\cos \frac{\pi v}{2} - 1 \right) \quad (31)$$

Substituting Equation 28, 29 and 30 into 22, gives:

$$\begin{aligned} \# = \frac{Et^3 \gamma}{24(1 + \mu)(1 - 2\mu)} & \left[(1 - \mu)h^2 r_x \right. \\ & + \frac{1}{\gamma^2} \left[h \cdot g + \frac{(1 - 2\mu)h^2}{2} + \frac{(1 - 2\mu)g^2}{2} \right] r_{xy} + \frac{(1 - \mu)g^2}{\gamma^4} r_y \\ & + 6(1 - 2\mu)\beta^2 \left([h^2 + \eta^2 + 2 \eta h] \cdot r_z + \frac{1}{\gamma^2} \cdot [g^2 + \eta^2 + 2 \eta g] \cdot r_{2z} \right) \\ & \left. - \frac{2qa^4 r_c \eta}{D^*} \right] \quad (32) \end{aligned}$$

Where:

$$r_x = \int_0^1 \int_0^1 \left(\frac{\partial^2 C}{\partial u^2} \right)^2 \partial u \partial v \quad (33)$$

$$r_{xy} = \int_0^1 \int_0^1 \left(\frac{\partial^2 C}{\partial u \partial v} \right)^2 \partial u \partial v \quad (34)$$

$$r_y = \int_0^1 \int_0^1 \left(\frac{\partial^2 C}{\partial v^2} \right)^2 \partial u \partial v \quad (35)$$

$$r_z = \int_0^1 \int_0^1 \left(\frac{\partial C}{\partial u} \right)^2 \partial u \partial v \quad (36)$$

$$r_{2z} = \int_0^1 \int_0^1 \left(\frac{\partial C}{\partial v} \right)^2 \partial u \partial v \quad (37)$$

$$r_c = \int_0^1 \int_0^1 C \partial u \partial v \quad (38)$$

Minimizing Equation 32 with respect to h gives:

$$\frac{1}{2\gamma^2} [g + h(1 - 2\mu)]r_{xy} + hr_x(1 - \mu) = -6(1 - 2\mu)\beta^2[h + \rho].r_z \quad (39)$$

Minimizing Equation 32 with respect to g gives:

$$\frac{1}{2\gamma^2} [h + g(1 - 2\mu)]r_{xy} + \frac{(1 - \mu)g}{\gamma^4} k_y = +\frac{6}{\gamma^2} (1 - 2\mu)\beta^2([g + \rho].r_{2z}) \quad (40)$$

Re-write the Equation (39) and (40) and simplifying to give:

$$h = \rho \frac{(k_{12}k_{23} - k_{13}k_{22})}{(k_{12}k_{12} - k_{11}k_{22})} \quad (41)$$

$$g = \rho \frac{(k_{12}k_{13} - k_{11}k_{23})}{(k_{12}k_{12} - k_{11}k_{22})} \quad (42)$$

Where;

$$k_{11} = (1 - \mu)r_x + \frac{1}{2\gamma^2} (1 - 2\mu)r_{xy} + 6(1 - 2\mu)\beta^2 r_z \quad (43)$$

$$k_{12} = k_{21} = \frac{1}{2\gamma^2} r_{xy}; \quad k_{13} = -6(1 - 2\mu)\beta^2 r_z \quad (44)$$

$$k_{22} = \frac{(1 - \mu)}{\gamma^4} r_y + \frac{1}{2\gamma^2} (1 - 2\mu)r_{xy} + \frac{6}{\gamma^2} (1 - 2\mu)\beta^2 r_{2z} \quad (45)$$

$$k_{23} = k_{32} = -\frac{6}{\gamma^2} (1 - 2\mu)\beta^2 r_{2z} \quad (46)$$

Minimizing Equation 32 with respect to \cap gives:

$$\frac{Et^3\gamma}{24(1+\mu)(1-2\mu)} \left[6(1-2\mu)\beta^2 \left([2\cap+2h].r_z + \frac{1}{\gamma^2} \cdot [2\cap+2g].r_{2z} \right) \right] - \frac{24wa^4r_c(1+\mu)(1-2\mu)}{Et^3} = 0 \quad (47)$$

$$\begin{aligned} & \frac{(1-2\mu)\beta^2 Et^3\gamma}{4(1+\mu)(1-2\mu)} \left\{ \left[\cap + \cap \frac{(k_{12}k_{23} - k_{13}k_{22})}{(k_{12}k_{12} - k_{11}k_{22})} \right] \cdot r_z \right. \\ & \quad \left. + \frac{1}{\beta^2} \cdot \left[\cap + \cap \frac{(k_{12}k_{13} - k_{11}k_{23})}{(k_{12}k_{12} - k_{11}k_{22})} \right] \cdot r_{2z} \right\} \\ & = \frac{wa^4r_c(1+\mu)(1-2\mu)\beta^3}{E} \end{aligned} \quad (48)$$

Factorizing Equations (48) and simplifying gives:

$$\cap = \frac{2q(1+\mu)(1-2\mu)\beta^3}{E} \left\{ \frac{ar_c}{(1-2\mu) \left(\frac{a}{t} \right)^2 \left(\left[1 + \frac{(k_{12}k_{23} - k_{13}k_{22})}{(k_{12}k_{12} - k_{11}k_{22})} \right] \cdot r_z + \frac{1}{\beta^2} \cdot \left[1 + \frac{(k_{12}k_{13} - k_{11}k_{23})}{(k_{12}k_{12} - k_{11}k_{22})} \right] \cdot r_{2z} \right)} \right\} \quad (49)$$

2.6 Exact Displacement and Stress Expression

By substituting the value of \cap in Equation 49 into Equation 28, the deflection equation after satisfying the boundary condition of CSFS plate is given as:

$$v = \cap (\sin \pi u) \cdot \left(\cos \frac{\pi v}{2} - 1 \right) \quad (50)$$

Similarly, the in-plane displacement along x-axis becomes:

$$p = \frac{(k_{12}k_{23} - k_{13}k_{22})}{(k_{12}k_{12} - k_{11}k_{22})} \left\{ \frac{12q(1+\mu)(1-2\mu)\beta^2 kr_c}{(1-2\mu) \left(\frac{a}{t} \right)^2 \left(\left[1 + \frac{(k_{12}k_{23} - k_{13}k_{22})}{(k_{12}k_{12} - k_{11}k_{22})} \right] \cdot r_z + \frac{1}{\beta^2} \cdot \left[1 + \frac{(k_{12}k_{13} - k_{11}k_{23})}{(k_{12}k_{12} - k_{11}k_{22})} \right] \cdot r_{2z} \right)} \right\} \frac{1}{E} \frac{\partial C}{\partial u} \quad (51)$$

$$p = \frac{12q(1+\mu)(1-2\mu)\beta^2}{E} \left(\frac{kMr_c}{L} \right) \frac{\partial C}{\partial u} \quad (52)$$

Where;

$$L = 6(1-2\mu)\beta^2 \left([1+h].r_z + \frac{1}{\gamma^2} \cdot [1+g].r_{2z} \right) \quad (50)$$

$$N = \frac{(r_{12}r_{23} - r_{13}r_{22})}{(r_{12}r_{12} - r_{11}r_{22})} \quad (50)$$

$$M = \frac{(r_{12}r_{13} - r_{11}r_{23})}{(r_{12}r_{12} - r_{11}r_{22})} \quad (50)$$

Similarly, the in-plane displacement along y-axis becomes;

$$q = \frac{12q(1 + \mu)(1 - 2\mu)\beta}{E} \left(\frac{kNr_c}{L} \right) \frac{\partial C}{\partial v} \quad (50)$$

The six stress elements after satisfying the boundary condition are presented in Equations (57) – (62) as:

$$\sigma_x = \frac{E}{(1 + \mu)(1 - 2\mu)} \left[\frac{k}{\beta} \cdot \frac{\partial^2 C}{\partial u^2} (1 - \mu) + \mu\beta^4 * \frac{12q(1 + \mu)(1 - 2\mu)}{E} \left(\frac{r_c}{L} \right) \frac{\partial C}{\partial k} + \frac{\mu k}{\gamma\beta} \cdot \frac{\partial^2 C}{\partial v^2} \right] \quad (50)$$

$$\sigma_y = \frac{E}{(1 + \mu)(1 - 2\mu)} \left[\frac{\mu k}{\beta} \cdot \frac{\partial^2 C}{\partial u^2} + \mu\beta^4 * \frac{12q(1 + \mu)(1 - 2\mu)}{E} \left(\frac{r_c}{L} \right) \frac{\partial C}{\partial k} + \frac{(1 - \mu)k}{\gamma\beta} \cdot \frac{\partial^2 C}{\partial v^2} \right] \quad (50)$$

$$\sigma_z = \frac{E}{(1 + \mu)(1 - 2\mu)} \left[\frac{\mu k}{\beta} \cdot \frac{\partial^2 C}{\partial u^2} + (1 - \mu)\beta^4 * \frac{12q(1 + \mu)(1 - 2\mu)}{\beta} \left(\frac{r_c}{L} \right) \frac{\partial C}{\partial k} + \frac{\mu k}{\gamma\beta} \cdot \frac{\partial^2 C}{\partial v^2} \right] \quad (50)$$

$$\tau_{xy} = \frac{E(1 - 2\mu)}{(1 + \mu)(1 - 2\mu)} \cdot \left[\frac{k}{2\beta} \cdot \frac{\partial^2 \partial C}{\partial u \partial v} + \frac{\beta^2 k}{2\alpha\gamma} \cdot \frac{12q(1 + \mu)(1 - 2\mu)}{E} \left(\frac{r_c}{L} \right) \frac{\partial^2 \partial C}{\partial u \partial v} \right] \quad (50)$$

$$\tau_{xz} = \frac{(1 - 2\mu)E}{(1 + \mu)(1 - 2\mu)} \cdot \left[\frac{1}{2} \frac{\partial C}{\partial u} + \frac{\beta^3}{2} * \frac{12q(1 + \mu)(1 - 2\mu)}{E} \left(\frac{r_c}{L} \right) \frac{\partial C}{\partial u} \right] \quad (50)$$

$$\tau_{yz} = \frac{(1 - 2\mu)E}{(1 + \mu)(1 - 2\mu)} \cdot \left[\frac{1}{2} \frac{\partial C}{\partial v} + \frac{\beta^3}{2\gamma} * \frac{12q(1 + \mu)(1 - 2\mu)}{E} \left(\frac{r_c}{L} \right) \frac{\partial C}{\partial v} \right] \quad (50)$$

3. Results and Discussion

This study has successfully combined the use of exact trigonometric functions, 3-D plate theory and direct variation approach to obtain the results of the non-dimensional values of displacements (w , u , and v), and stresses (σ_x , σ_y , τ_{xy} , τ_{xz} , and τ_{yz}) for a three-dimensional isotropic CSFS thick plate subjected to uniformly distributed load. The effects of displacements and stresses on span-to-thickness ratio of 5, 10, 15, 20, 25, 100 and 1000, are presented in Figures 3 to 6, at length-to-breadth ratio of 1.0 and 2.0 respectively. To show the distinctiveness of this model, the outcome of the present study was compared with the results of same plate obtained by different scholars.

Figures 3 and 4 shows the effect of increasing the span-to-thickness ratio (a/t) on the out-of-plane and in-plane displacements of the plate structure. It can be observed that the out-of-plane displacement values (w) decreased in the positive direction as the span-to-depth ratio increased. But the out-of-plane displacement values increased at each aspect ratio as the length-to-breadth ratio increased. The reductions were very crystal clear at $a/t \leq 20$ (thick plate region), slightly visible at $20 \leq a/t \leq 45$ (Moderately-thick plate region), but becomes very little and almost negligible at $a/t \geq 50$ (thin-plate zone). This indicates that deflection is more pronounced for thick plates than thin plates. This also implies that there are chances for failure in the plate structure if the plate width is increased. The tendency of this failure can be alleviated by reducing the plate width.

In Figures 5 and 6, it is also observed that the in-plane displacements (u & v) increased negatively as the span-depth ratio increased. This implies that the effects of in-plane displacements are less on thick plates but more on thin plates. As the longest-breadth ratio increased from 1.0 to 2.0, this effect increased at each span-to-depth ratio. 0.006069 and 0.009791, 0.005513 and 0.008855 were the maximum and minimum values for the deflections at length-to-width ratio of 1.0 and 2.0 respectively. Looking critically at the values obtained from this work, it can be deduced that this model and its exact trigonometric shape functions are quite adequate for thick plate analysis.

From Figures 5 and 6, it is observed that the normal stresses (σ_x , and σ_y) decreased positively as the span-to-thickness ratio increased for each length-to-breadth ratio. In figure 5, the shear stresses (τ_{xz} , and τ_{yz}) also decreased positively as the span-to-depth ratio increased; except for τ_{xy} , which increased negatively. In Figure 6, at a length - breadth ratio of 2.0, shear stress (τ_{xz}) decreased positively while the shear stresses (τ_{xy} , and τ_{yz}) increased negative. These identical properties of the material represented in the graphs confirms that the plates are isotropic. The figures show that the span-to-depth ratio between 5 and 20 varies between 0.006069 and 0.005548, 0.009791 and 0.008914 respectively with a constant decreased value of 0.000521 and 0.000877 in each case for the deflections in the plate structure. As they varied very much from zero, they can be considered as thick plates. Span-thickness ratios between 50 and 1000 with 0.005519 and 0.005513, 0.008864 and 0.00855 as out-of-plane displacement values in Tables 1 and 2 respectively; decreased to a constant value of 0.000006 and 0.000009 for each. This variation in deflection which is approximately zero justifies their categorization as thin plates.

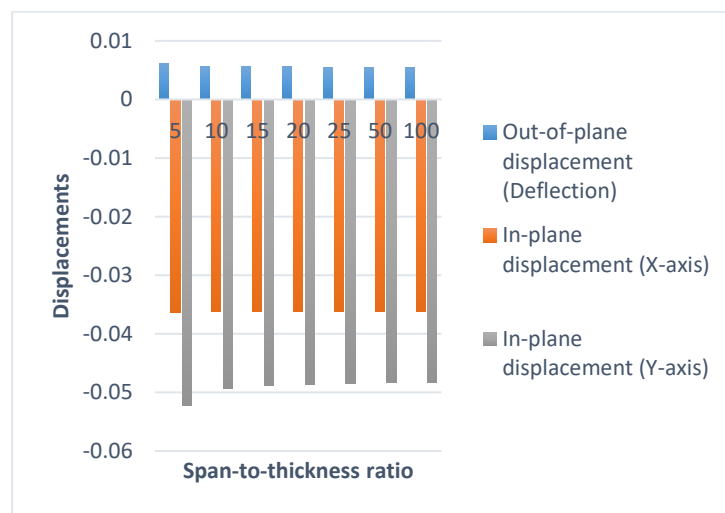


Figure 3: Variation of displacements with span-to-thickness ratio for length to breadth of 1.0

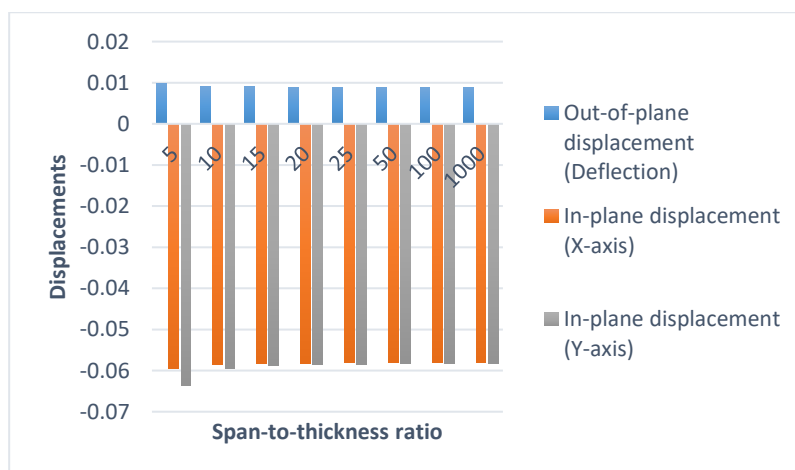


Figure 4: Variation of displacements with span-to-thickness ratio for length to breadth of 2.0

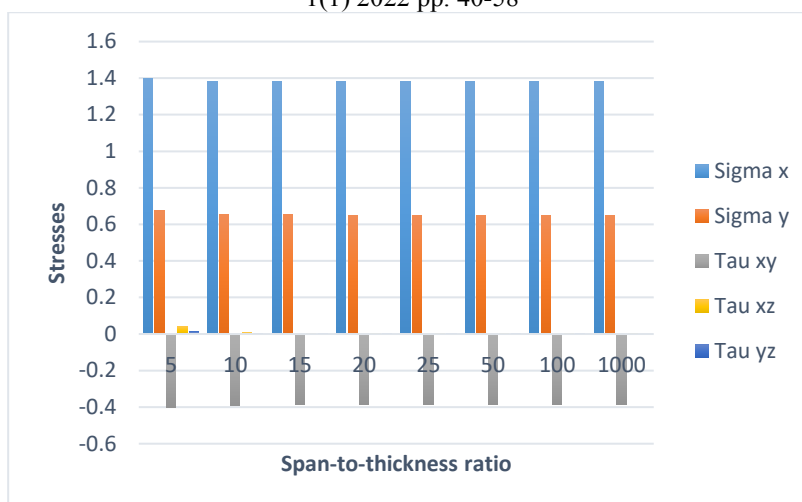


Figure 5: Variation of stresses with span-to-thickness ratio for length to breadth of 1.0

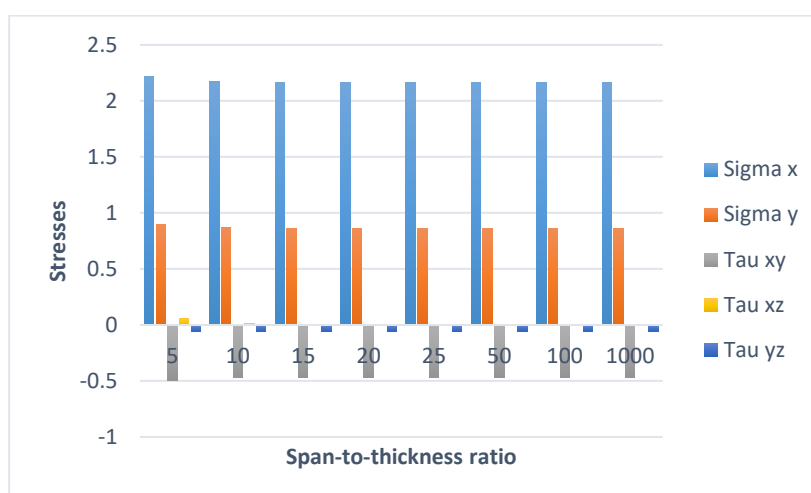


Figure 6: Variation of stresses with span-to-thickness ratio for length to breadth of 2.0

From Table 1 and Figure 7, it is confirmed that the refined plate theories which was employed by other scholars' overestimate or underestimate the deflection in the plate structure which makes their solution unrealistic compared to 3-D solve. This implies that RPTs are quite coarse for the analysis of thick plate. 3-D analysis ensures accuracy and exact solution for a three-dimensional plate problem. These scholars failed to apply trigonometric function which gives a close-form solution than polynomial whose exact function tends to infinity.

Table 1: Percentage difference between the values of non-dimensional center deflection of CSFS rectangular thick plates from present and past studies at different span to thickness ratio for length to width ratio of 1.0.

$\beta = a/t$	Present Work [P.W]	Onyeka (2021) [40]	Gwarah (2019) [48]	Percentage difference between [P.W] & [40]	Percentage difference between [P.W] & [48]
5	0.00607	0.00609	0.00672	0.2966	10.6443
10	0.00565	0.00537	0.00593	4.9876	4.8638
20	0.00555	0.00520	0.00573	6.3446	3.2805

30	0.00553	0.00516	0.00569	6.6196	2.9662
40	0.00552	0.00515	0.00568	6.7005	2.8613
50	0.00552	0.00515	0.00567	6.7585	2.8085
60	0.00553	0.00514	0.00567	6.7609	2.7914
70	0.00552	0.00514	0.00567	6.7803	2.7737
80	0.00551	0.00514	0.00567	6.7815	2.7743
90	0.00551	0.00514	0.00567	6.7827	2.7748
100	0.00551	0.00514	0.00567	6.8009	2.7566
				5.91%	3.75%
Average Percentage difference					
Total Percentage difference				4.83%	

The present study was analogized to Onyeka (2021) and Gwarah (2019) as shown in Table 1 and they differed in their percentage difference by 5.91% and 3.75% respectively. These differences occurred on account of the polynomial 2D-RPT model employed by both authors using exact and assumed displacement functions respectively. The slightly higher and lower variations presented in Figure 3 revealed the disparity between the refined plate theories and the present theory as the overestimate and underestimate the deflections in the plate structure. The correctness of the close-form solution obtained from the present work amplifies the need to apply an exact trigonometric function in analyzing the bending of a typical 3-D rectangular thick plate subjected to same boundary and loading condition.

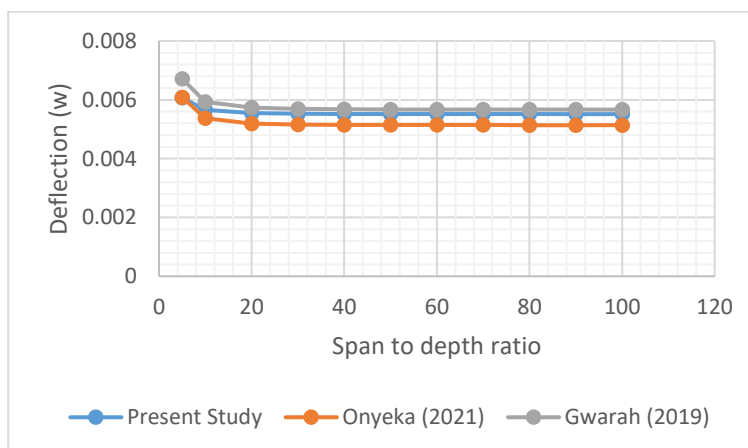


Figure 7: Variation of central deflection of CSFS square thick plates with span-thickness ratio

The gross average percentage difference between the previous studies and this work is 4.83%. This signifies that at about 95% confidence level, the values obtained in this study are equal to those of past studies. This confidence level certifies that the present model can be employed with conviction for stress and displacement analysis of CSFS thick rectangular plates.

4. Conclusion

The stress and bending analysis of thick rectangular plates was investigated using the 3D trigonometric theory and the following conclusion was reached:

- i) The 3-D model has an accurate prediction than those of RPT and CPT due to the consideration of all the six strains and stresses components, with the inclusion of modulus of elasticity and other engineering properties of the plate structure.

- ii) The efficacy of this model is validated based on the percentage difference recorded for square plate deflections relative to previous studies. It was confirmed that 3-D analogy is needed for the three-dimensional thick plate analysis as 2-D RPT provides an inappropriate solution.
- iii) The trigonometric displacement functions obtained from the governing equations are exact and consistent. With certainty, they can be applied to the analysis of any thick plate under equivalent loading and support conditions.

Nomenclature

k	non-dimensional parameters of z-axis
u	non-dimensional parameters of x-axis
v	non-dimensional parameters of y-axis
t	thickness of the plate,
p	in-plane displacement along x-axis
q	in-plane displacement along y-axis
h	coefficient of shear deformation along x-axis of the plate
g	coefficient of shear deformation along y-axis of the plate
ε_x	normal strain along x-axis
ε_y	normal strain along y-axis
ε_z	normal strain along z-axis
γ_{xy}	shear strain in the plane parallel to the x-y plane
γ_{xz}	shear strain in the plane parallel to the x-z plane
γ_{yz}	shear strain in the plane parallel to the y-z plane
τ_{xy}	shear stress in the plane parallel to the x-y plane
τ_{xz}	shear stress in the plane parallel to the x-z plane
τ_{yz}	shear stress in the plane parallel to the y-z plane
E	modulus of elasticity
μ	Poisson's ratio
\bar{A}	Potential energy of the plate
\bar{E}	Strain energy of the plate
$\bar{\Theta}$	External work done on the plate
C	Plate's shape function
w	Uniformly distributed load
U	Deflection function of the plate
\cap	Coefficient of deflection
ϕ_x	Coefficient of shear deformation along x-axis
ϕ_y	Coefficient of shear deformation along y-axis
p	In-plane displacement along x-axis
q	In-plane displacement along y-axis
β	Span-thickness ratio
α	Aspect ratio

References

- [1] F. C. Onyeka (2019). Direct analysis of critical lateral load in a thick rectangular plate using refined plate theory. International Journal of Civil Engineering and Technology, vol. 10, no. 5, pp. 492-505.
- [2] F. C. Onyeka, B. O. Mama, C. D. Nwa-David (2022). Application of Variation Method in Three-Dimensional Stability Analysis of Rectangular Plate Using Various Exact Shape Functions. Nigerian Journal of Technology (NIJOTECH), Vol. 41 No. 1, pp. 8-20, 2022. DOI: <http://dx.doi.org/10.4314/njt.v41i1.2>

- [3] F. C. Onyeka, B. O. Mama, C. D. Nwa-David (2022). Static and Buckling Analysis of a Three-Dimensional (3-D) Rectangular Thick Plates Using Exact Polynomial Displacement Function. *European Journal of Engineering and Technology Research*, Vol. 7, No. 2, pp. 29-35. DOI: <http://dx.doi.org/10.24018/ejeng.2022.7.2.2725>
- [4] F. C. Onyeka and O. T. Edozie (2020). Application of Higher Order Shear Deformation Theory in the Analysis of thick Rectangular Plate. *International Journal on Emerging Technologies*, Vol. 11, No. 5, pp. 62–67.
- [5] F. C. Onyeka, C. D. Nwa-David, E. E. Arinze (2021). Structural Imposed Load Analysis of Isotropic Rectangular Plate Carrying a Uniformly Distributed Load Using Refined Shear Plate Theory, *FUOYE Journal of Engineering and Technology (FUOYEJET)*, Vol. 6, No. 4, pp. 414-419. DOI: <http://dx.doi.org/10.46792/fuoyejet.v6i4.719>
- [6] C. H. Aginam, C. A. Chidolue and C. A. Ezeagu (2012). Application of direct variational method in the analysis of isotropic thin rectangular plates. *ARNP Journal of Engineering and Applied Sciences*, vol. 7, no. 9, pp. 1128-1138.
- [7] F. C. Onyeka, C. D. Nwa-David, T. E. Okeke (2022). Study on Stability Analysis of Rectangular Plates Section Using a Three-Dimensional Plate Theory with Polynomial Function. *Journal of Engineering Research and Sciences*, Vol. 1, No. 4, pp. 28-37. DOI: <https://dx.doi.org/10.55708/js0104004>
- [8] F. C. Onyeka (2022). Stability Analysis of Three-Dimensional Thick Rectangular Plate Using Direct Variational Energy Method. PhD Thesis University of Nigeria, Nsukka, *Journal of Advances in Science and Engineering*, 6–t, pp.1–78. DOI: <https://doi.org/10.37121/jase.v6i2.187>
- [9] E. Ventsel, T. Krauthammer (2001). *Thin plates and shells theory, analysis and applications*. Maxwell Publishers Inc; New York.
- [10] J. N. Reddy (2006). *Classical theory of plates,*” In *Theory and Analysis of Elastic Plates and Shells*, CRC Press. DOI: 10.1201/9780849384165-7
- [11] K. Chandrashekhara (2001). *Theory of plates*. University Press (India) Limited.
- [12] F. C. Onyeka, B. O. Mama, C. D. Nwa-David (2022). Analytical Modelling of a Three-Dimensional (3D) Rectangular Plate Using the Exact Solution Approach. *IOSR Journal of Mechanical and Civil Engineering (IOSR-JMCE)*, Vol. 19, No. 1, pp. 76-88. DOI: 10.9790/1684-1901017688
- [13] F. C. Onyeka, T. E. Okeke, C. D. Nwa-David (2022). Buckling Analysis of a Three-Dimensional Rectangular Plates Material Based on Exact Trigonometric Plate Theory. *Journal of Engineering Research and Sciences*, Vol. 1, no. 3, pp. 106-115. DOI: <https://dx.doi.org/10.55708/js0103011>
- [14] F. C. Onyeka, B. O. Mama and T. E. Okeke, C. D. (2022). Exact three-dimensional stability analysis of plate using a direct variational energy method. *Civil Engineering Journal*, Vol. 8, no. 1, pp. 60-80. DOI: <http://dx.doi.org/10.28991/CEJ-2022-08-01-05>
- [15] S. P. Timoshenko, and S. Woinowsky-krieger (1970). *Theory of plates and shells*, (2nd Ed.). Mc Graw-Hill Book Co. P.379, Singapore.
- [16] G. Kirchhoff (1859). U^{ber} das Gleichgewicht und die Bewegung einer elastischen Scheibe. *J. Reine Angew. Math.*, Vol. 40, pp. 51-88.
- [17] R. D. Mindlin (1951). Influence of rotary inertia and shear on flexural motions of isotropic elastic plates. *Trans. ASME J. Appl. Mech.*, Vol. 18, pp. 31-38.
- [18] E. Reissner (1945). The effect of transverse shear deformation on the bending of elastic plates. *Trans ASME J. Appl. Mech.*, Vol. 12, no. 2, pp. 69-77.
- [19] J. N. Reddy (1984). A simple higher-order theory for laminated composite plates. *Trans. ASME J. Appl. Mech.*, Vol. 51, pp. 745-752.
- [20] J. N. Reddy, N. D. Phan (1985). Stability and vibration of isotropic, orthotropic and laminated plates according to a higher-order shear deformation theory. *J. Sound Vib.*, Vol. 98, no. 2, pp. 157-170.
- [21] F. C. Onyeka and B. O. Mama (2021). Analytical study of bending characteristics of an elastic rectangular plate using direct variational energy approach with trigonometric function. *Emerging Science Journal*, vol. 5, no. 6, pp. 916–926. DOI: <http://dx.doi.org/10.28991/esj-2021-01320>
- [22] F. C. Onyeka, B.O. Mama, C.D Nwa-David, T.E. Okeke (2022). Exact Analytic Solution for Static Bending of 3-D Plate under Transverse Loading. *Journal of Computational Applied Mechanics*. DOI: 10.22059/JCAMECH.2022.342953.721
- [23] F. C. Onyeka and T. E. Okeke (2021). Elastic bending analysis exact solution of plate using alternative I refined plate theory. *Nigerian Journal of Technology*, Vol. 40, no. 6, pp. 1018 –1029. DOI: <http://dx.doi.org/10.4314/njt.v40i6.4>
- [24] F. C. Onyeka, T. E. Okeke, J. Wasiu (2020). Strain–Displacement Expressions and their Effect on the Deflection and Strength of Plate. *Advances in Science, Technology and Engineering Systems Journal*, Vol. 5, no. 5, pp. 401-413.
- [25] C. C. Ike (2017). Equilibrium Approach in the Derivation of Differential Equation for Homogeneous Isotropic Mindlin Plates. *Nigerian Journal of Technology (NIJOTECH)*, Vol. 36, no. 2, pp. 346-350. DOI: <https://doi.org/10.4314/njt.v36i2.4>

- [26] N. N. Osadebe, C. C. Ike, H. N. Onah, C. U. Nwoji and F. O. Okafor (2016). Application of Galerkin-Vlasov Method to the Flexural Analysis of Simply Supported Rectangular Kirchhoff Plates under Uniform Loads. *Nigerian Journal of Technology (NIJOTECH)*, Vol. 35, no. 4, pp. 732-738. DOI: <https://doi.org/10.4314/njt.v35i4.7>
- [27] C. U. Nwoji, B. O. Mama, C. C. Ike and H. N. Onah (2017). Galerkin-Vlasov method for the flexural analysis of rectangular Kirchhoff plates with clamped and simply supported edges. *IOSR Journal of Mechanical and Civil Engineering (IOSR JMCE)*, Vol. 14, no. 2, pp. 61-74. DOI: <https://doi.org/10.9790/1684-1402016174>
- [28] R. Szilard (2004). *Theories and Applications of Plates Analysis: Classical, Numerical and Engineering Methods*. John Wiley and Sons Inc.
- [29] H. N. Kapadiya, A. D. Patel (2015). Review of Bending Solutions of thin Plates". *International Journal of Scientific Research and Development (IJSRD)*, Vol. 3, no. 3, pp. 1709-1712.
- [30] B. O. Mama, C. U. Nwoji, C. C. Ike and H. N. Onah (2017). Analysis of Simply Supported Rectangular Kirchhoff Plates by the Finite Fourier Sine Transform Method. *International Journal of Advanced Engineering Research and Science (IJAERS)*, Vol. 4, no. 3, pp. 285-291. DOI: <https://doi.org/10.22161/ijaers.4.3.44>
- [31] N. G. Iyengar (1988). *Structural Stability of Columns and Plates*. New York: Ellis Horwood Limited.
- [32] F. C. Onyeka and E. T. Okeke (2021). Analytical Solution of Thick Rectangular Plate with Clamped and Free Support Boundary Condition Using Polynomial Shear Deformation Theory. *Advances in Science, Technology and Engineering Systems Journal*, Vol. 6, no. 1, pp. 1427-1439. doi: 10.25046/aj0601162
- [33] F. C. Onyeka, F. O. Okafor, H. N. Onah (2021). Application of a New Trigonometric Theory in the Buckling Analysis of Three-Dimensional Thick Plate. *International Journal of Emerging Technologies*, Vol. 12, no. 1, pp. 228-240.
- [34] F. C. Onyeka, F. O. Okafor, H. N. Onah (2021). Buckling Solution of a Three-Dimensional Clamped Rectangular Thick Plate Using Direct Variational Method. *IOSR Journal of Mechanical and Civil Engineering (IOSR-JMCE)*, vol. 18, no. 3 Ser. III, pp. 10-22. doi: 10.9790/1684-1803031022
- [35] R. A. Shetty, S. A. Deepak, K. K. Sudheer, G. L. Dushyanthkumar (2022). Thick Plate Bending Analysis using a Single Variable Simple Plate Theory, *Materials Today: Proceedings*, Vol. 54, no. 2, pp. 191-195. DOI: <https://doi.org/10.1016/j.matpr.2021.08.289>
- [36] D. P. Bhaskar, A. G. Thakur, I. I. Sayyad and S. V. Bhaskar (2021). Numerical Analysis of Thick Isotropic and Transversely Isotropic Plates in Bending using FE Based New Inverse Shear Deformation Theory. *International Journal of Automotive and Mechanical Engineering (IJAME)*, Vol. 18, no. 3, pp. 8882-8894. DOI: <https://doi.org/10.15282/ijame.18.3.2021.04.0681>
- [37] A. S. Sayyada, and Y. M. Ghugal (2012). Bending and free vibration analysis of thick isotropic plates by using exponential shear deformation theory. *Applied and Computational Mechanics* Vol. 6, pp. 65-82.
- [38] J. L. Mantari and C. G. Soares (2012). Bending Analysis of Thick Exponentially Graded Plates using a new Trigonometric Higher Order Shear Deformation Theory. *Composite Structures*, Vol. 94, no. 6, pp. 1991-2000. DOI: <https://doi.org/10.1016/j.compstruct.2012.01.005>
- [39] F. Y. Tash and B. N. Neya (2020). An Analytical Solution for Bending of Transversely Isotropic Thick Rectangular Plates with Variable Thickness. *Applied Mathematical Modelling*, Vol. 77, no. 2, pp. 1582-1602. DOI: <https://doi.org/10.1016/j.apm.2019.08.017>
- [40] H. T. Thai, D. H. Choi (2013). Analytical Solutions of Refined Plate Theory for Bending, Buckling and Vibration Analyses of Thick Plates. *Applied Mathematical Modelling*, Vol. 37, pp. 8310-8323. DOI: <http://dx.doi.org/10.1016/j.apm.2013.03.038>
- [41] Y. Zhong and Q. Xu (2017). Analysis Bending Solutions of Clamped Rectangular Thick Plate. *Mathematical Problems in Engineering*, Vol. 2017, pp. 1-6. DOI: <https://doi.org/10.1155/2017/7539276>
- [42] Y. M. Ghugal, P. D. Gajbhiye (2016). Bending Analysis of Thick Isotropic Plates by Using 5th Order Shear Deformation Theory. *Journal of Applied and Computational Mechanics*, Vol. 2, no. 2, pp. 80-95. DOI: 10.22055/jacm.2016.12366
- [43] O. M. Ibearugbulem, J. C. Ezech, L. O. Ettu, L. S. Gwarah (2018). Bending Analysis of Rectangular Thick Plate Using Polynomial Shear Deformation Theory, *IOSR Journal of Engineering (IOSRJEN)*, Vol. 8, no. 9, pp. 53-61.
- [44] F. C. Onyeka (2021). Effect of Stress and Load Distribution Analysis on an Isotropic Rectangular Plate. *Arid Zone Journal of Engineering, Technology & Environment*, Vol. 17, no. 1, pp. 9-26.
- [45] J. C. Ezech, O. M. Ibearugbulem, L. O. Ettu, L. S. Gwarah, I. C. Onyechere (2018). Application of shear deformation theory for analysis of CCCS and SSFS rectangular isotropic thick plates. *Journal of Mechanical and Civil Engineering (IOSR-JMCE)*, Vol. 15, no. 5, pp. 33 - 42. DOI: 10.9790/1684-1505023342
- [46] O. M. Ibearugbulem, U. C. Onwuegbuchulem, C. N. Ibearugbulem (2021). Analytical Three-Dimensional Bending Analyses of Simply Supported Thick Rectangular Plate. *International Journal of Engineering Advanced Research (IJEAR)*, Vol. 3, no. 1, pp. 27-45.
- [47] A. Y. Grigorenko, A. S. Bergulev, S. N. Yaremchenko (2013). Numerical solution of bending problems for rectangular plates. *International Applied Mechanics*, Vol. 49, no. 1, pp. 81 - 94. DOI: <https://doi.org/10.1007/s10778-013-0554-1>

- [48] L. S. Gwarah (2019). Application of shear deformation theory in the analysis of thick rectangular plates using polynomial displacement functions. PhD Thesis Presented to the School of Civil Engineering, Federal University of Technology, Owerri, Nigeria.